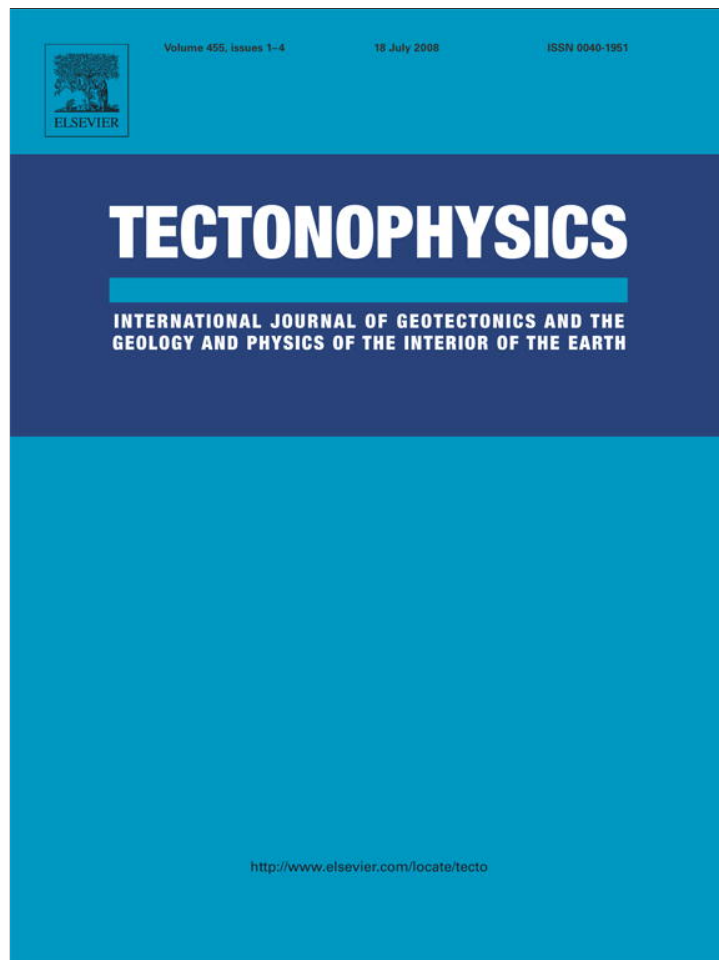


Provided for non-commercial research and education use.
Not for reproduction, distribution or commercial use.



This article appeared in a journal published by Elsevier. The attached copy is furnished to the author for internal non-commercial research and education use, including for instruction at the authors institution and sharing with colleagues.

Other uses, including reproduction and distribution, or selling or licensing copies, or posting to personal, institutional or third party websites are prohibited.

In most cases authors are permitted to post their version of the article (e.g. in Word or Tex form) to their personal website or institutional repository. Authors requiring further information regarding Elsevier's archiving and manuscript policies are encouraged to visit:

<http://www.elsevier.com/copyright>



Contents lists available at ScienceDirect

Tectonophysics

journal homepage: www.elsevier.com/locate/tecto

The role of the Kazakhstan orocline in the late Paleozoic amalgamation of Eurasia

Alexandra Abrajevitch^a, Rob Van der Voo^{a,*}, Mikhail L. Bazhenov^b,
Natalia M. Levashova^b, Phil J.A. McCausland^c^a Department of Geological Sciences, University of Michigan, Ann Arbor, Michigan 48109-1005, USA^b Geological Institute, Academy of Sciences of Russia, Pyzhevsky Lane, 7, Moscow, 109017, Russia^c The University of Western Ontario, 1151 Richmond Street, London, Ontario, Canada N6A 5B7

ARTICLE INFO

Article history:

Received 6 February 2008
Received in revised form 5 May 2008
Accepted 8 May 2008
Available online 16 May 2008

Keywords:

Paleomagnetism
Kazakhstan
Oroclinal bending
Late Paleozoic
Paleogeography

ABSTRACT

The Kazakhstan orocline, a horseshoe-shaped belt with volcanic arcs of Devonian (external) and late Paleozoic (internal) age, is thought to have formed as a result of convergence between the cratons of Siberia, Baltica and Tarim leading to the amalgamation of Eurasia. Paleomagnetic and geologic data indicate that in the Middle Devonian the arc, which is now strongly curved, was nearly straight near the northwest–southeast trending volcanic margin of a Kazakhstanian continent. To constrain the age of oroclinal bending we conducted a paleomagnetic study of Late Carboniferous to Late Permian subduction-related volcanics from the middle (NW) and north-eastern (NE) limbs of the orocline. Our new results indicate that the rotation of the middle arm of the orocline was essentially completed by the earliest Permian, while the NE arm probably was still ~50° short of its final orientation with respect to Baltica. The rotation of, or rotation within, the NE arm was completed by the Late Permian.

The paleomagnetic data constraining the timing and rotation patterns lead us to propose the following scenario for the bending of the Kazakhstan orocline. The orogenic deformation scenario began in the Late Devonian when an initial collision with Tarim pinned Kazakhstanian's southern corner, while a dextral shear motion and a considerable clockwise rotation of Siberia dragged its northern end. Relative convergence between Siberia and Tarim caused initial buckling of the Kazakhstanian continental element trapped between them, subdividing the belt into three (SW, NW, NE) segments. Continued subduction under the established limbs of the orocline with an estimated outward-directed subduction velocity of well less than 1 cm/yr gradually led to closure of the intervening Junggar–Balkhash oceanic basin and tightening of the orocline.

© 2008 Elsevier B.V. All rights reserved.

1. Introduction

Oroclines, or curved bends of map-view tectonic elements, are common features of continental crust and may have played an important role in the making of continental lithosphere (Van der Voo, 2004). In its original definition by Carey (1955), the word orocline characterized an originally linear fold and thrust belt that became curved during subsequent deformations. The definition has since evolved for some authors to include any elongate lithospheric element, such as terranes, individual thrust sheets, magmatic arcs or sea-mount chains, as long as they have a significant degree of curvature (e.g., Johnston, 2004). Rotations within these elongated lithospheric elements have been found to develop in response to a variety of boundary conditions, ranging from local variations in the configuration of colliding terranes to regional changes in the stress-

field (for a comprehensive review on mechanisms driving oroclinal bending see Weil and Sussman (2004)). A particular mechanism and its inherent boundary conditions for bending may be deduced from the kinematics of the curvature formation.

The Kazakhstan orocline – a pair of concentric horseshoe-shaped volcanic belts in Central Kazakhstan (Fig. 1) – formed during the amalgamation of Eurasia; the ultimate cause of the bending is thought to be the convergence of the large cratonic blocks of Baltica, Siberia and Tarim (e.g. Zonenshain et al., 1990; Şengör et al., 1993; Van der Voo, 2004). Hence, the timing and pattern of rotations during the oroclinal orogeny could provide important kinematic constraints on the relative movements of these cratons prior to their amalgamation.

Previous paleomagnetic studies of the Kazakhstan orocline confined the timing of the oroclinal orogeny to an interval between the Middle Devonian (when the arc was still straight; Abrajevitch et al., 2007) to the Late Permian (the bending was essentially over; Levashova et al., 2003). To better understand the final stages of the bending and the geodynamic constraints this puts on the motion of the converging Baltica, Siberia and Tarim cratons, we studied a set of Upper Carboniferous to Upper Permian rocks at two localities from the

* Corresponding author. Tel.: +1 734 764 8322; fax: +1 734 763 4690.

E-mail addresses: alexabra@umich.edu (A. Abrajevitch), voo@umich.edu (R. Van der Voo), mibazh@mail.ru (M.L. Bazhenov), namile2007@rambler.ru (N.M. Levashova), pmccausl@uwo.ca (P.J.A. McCausland).

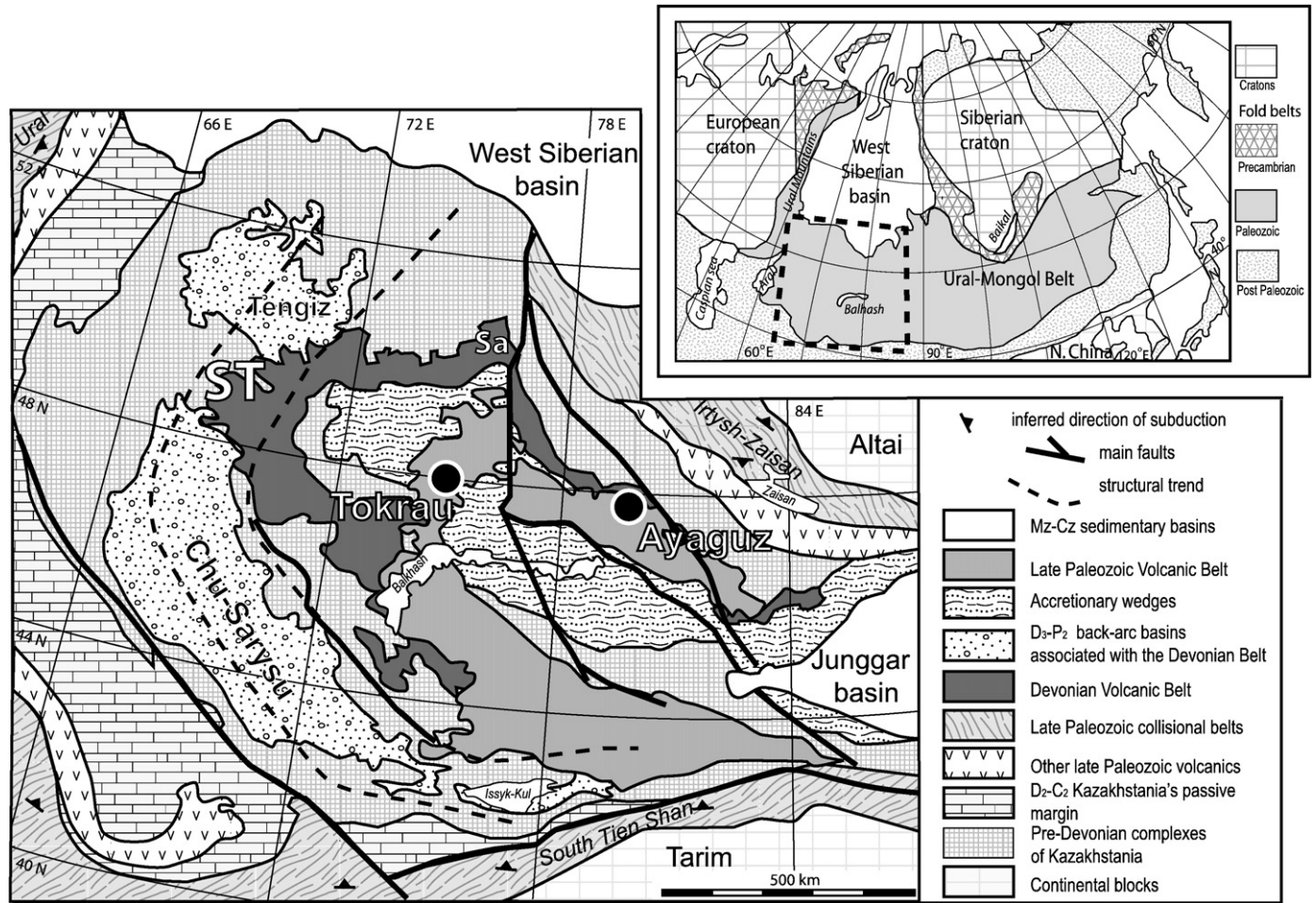


Fig. 1. Inset: Schematic map of Eurasia, showing the location of the Kazakhstan study area, wedged in between the European craton ("Baltica") and Siberia. The main map shows a tectonic interpretation of the study area, after Windley et al. (2007). D = Devonian, C = Carboniferous, P = Permian, Mz = Mesozoic, Cz = Cenozoic. Subscripts 2, 3 refer to Middle, Late. Sampling localities at Ayaguz and Tokrau are shown by large filled circles. The hinge zones of the Devonian volcanic belt, as mentioned in the text, are labeled Sa (Spassk anticlinorium) and ST (Sarysu–Tengiz uplift).

middle (locality Tokrau) and north-eastern (locality Ayaguz) arms of the curved structure (Fig. 1).

2. The tectonics of Kazakhstan and adjacent areas

In the Early and Middle Devonian, the areas to the west and southwest of the Devonian volcanic belt (Fig. 1) were above sea level, as indicated by continental red beds and subaerial volcanics. Marine sedimentation started in the Late Devonian and continued for most of Early Carboniferous time. These sediments consist of shallow-water limestones and clastic sediments; some marker horizons can be traced over hundreds of kilometers. From the end of the Early Carboniferous, clastic sedimentation, with rare shallow-marine and lacustrine interbeds, continued locally until Late Permian time. On the whole, the Early Devonian through Late Permian geologic record is usually interpreted as resulting from accumulation under subaerial or shallow-marine conditions. The complete lack of deep-water sediments, ophiolites, or sutures led most geologists to conclude that this part of Kazakhstan was one large continental mass during the second half of the Paleozoic.

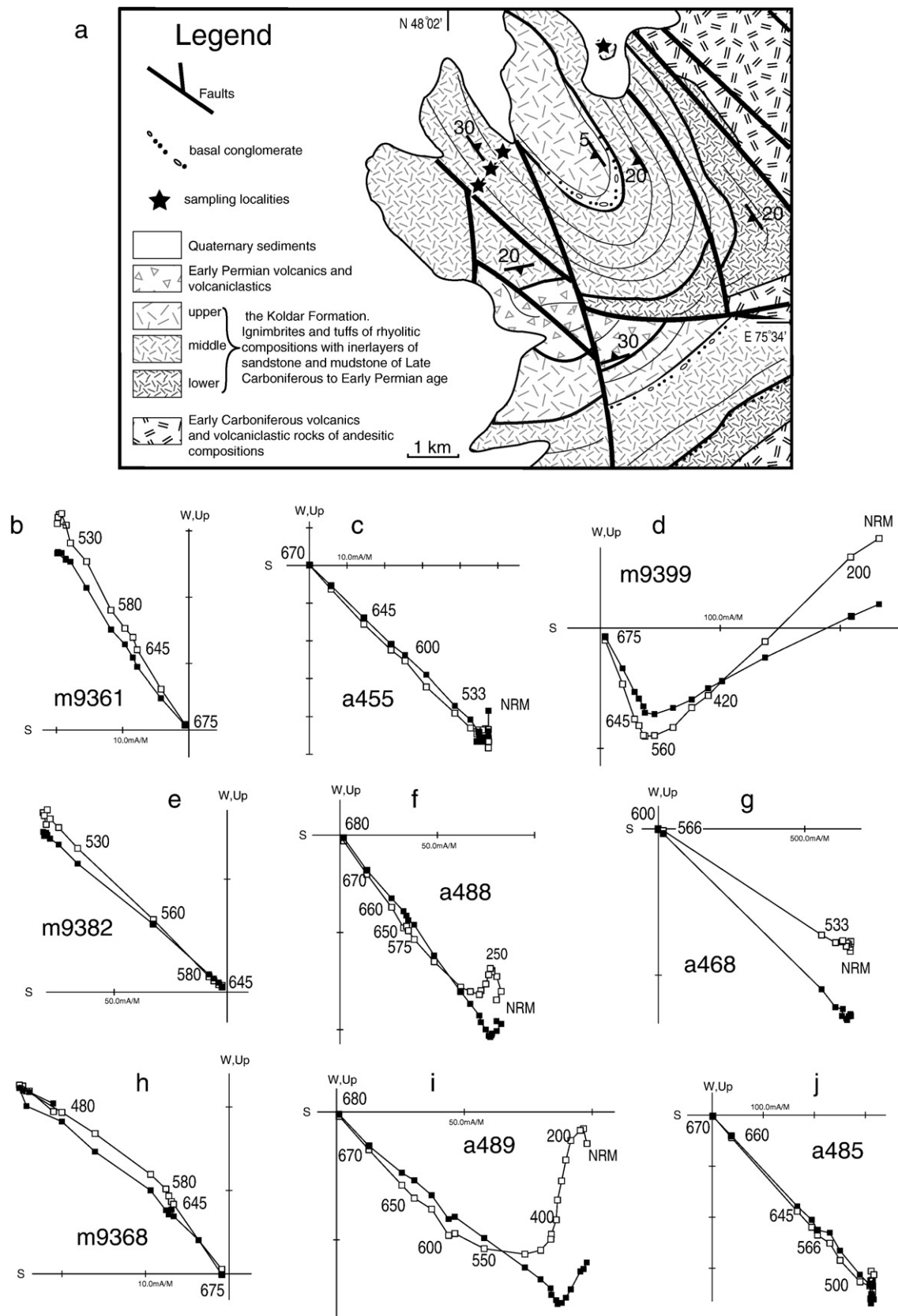
The situation is less clear to the north and northeast of the Devonian belt, where Devonian and younger rocks are less common and the record is less complete. Even there, however, the Devonian is represented by continental red beds of limited thickness, while deep-sea sediments are absent altogether. Despite numerous faults dissecting this area, none was ever regarded as a suture of Devonian or younger age.

Hence it is likely that the above territories formed a single continent (Kazakhstan block or microcontinent, also called Kazakhstania) at least since the Early Devonian. For instance, a single landmass is shown on such different reconstructions as those of Şengör and Natal'in (1996) and Filippova et al. (2001). Strong and laterally variable late Paleozoic deformation is agreed to by all scientists discussing the tectonics of this microcontinent, so Kazakhstania was not a rigid block. The scale and character of the deformation within Kazakhstan, however, remain controversial.

Kazakhstania is located in the center of the Eurasian continent and is made of crust stabilized during the Paleozoic that is sandwiched between the old cratons of Siberia, Baltica and Tarim (Fig. 1). Kazakhstania was assembled by accretion of various blocks with Precambrian crust, island arc fragments, and accretionary complexes. The mechanism of the early Paleozoic assembly and paleogeographic origin of the fragments comprising Kazakhstania are a matter of contention; proposed models range from collision of microcontinents that were originally separated by oceanic basins and multiple island arcs (Mossakovsky et al., 1993; Didenko et al., 1994; Dobretsov et al., 1995; Filippova et al., 2001; Windley et al., 2007), to forearc accretion and oroclinal bending of a single, long-lived subduction system (Şengör and Natal'in, 1996). Many models agree, though, that by middle Paleozoic time, these fragments coalesced into a single continental block, although the shape and origin of terranes incorporated in this block remain contentious (see for example, Şengör and Natal'in, 1996; Filippova et al., 2001; Windley et al., 2007). From the early Devonian onward, significant

subduction of oceanic (“Junggar–Balkhash”) lithosphere occurred underneath this continental element and led to the Devonian and younger volcanic arcs of Fig. 1. Carboniferous–Permian final collisions

with the surrounding Baltica, Siberia and Tarim cratons were probably preceded by limited subduction in locations at the three external sides of the orocline (Fig. 1).



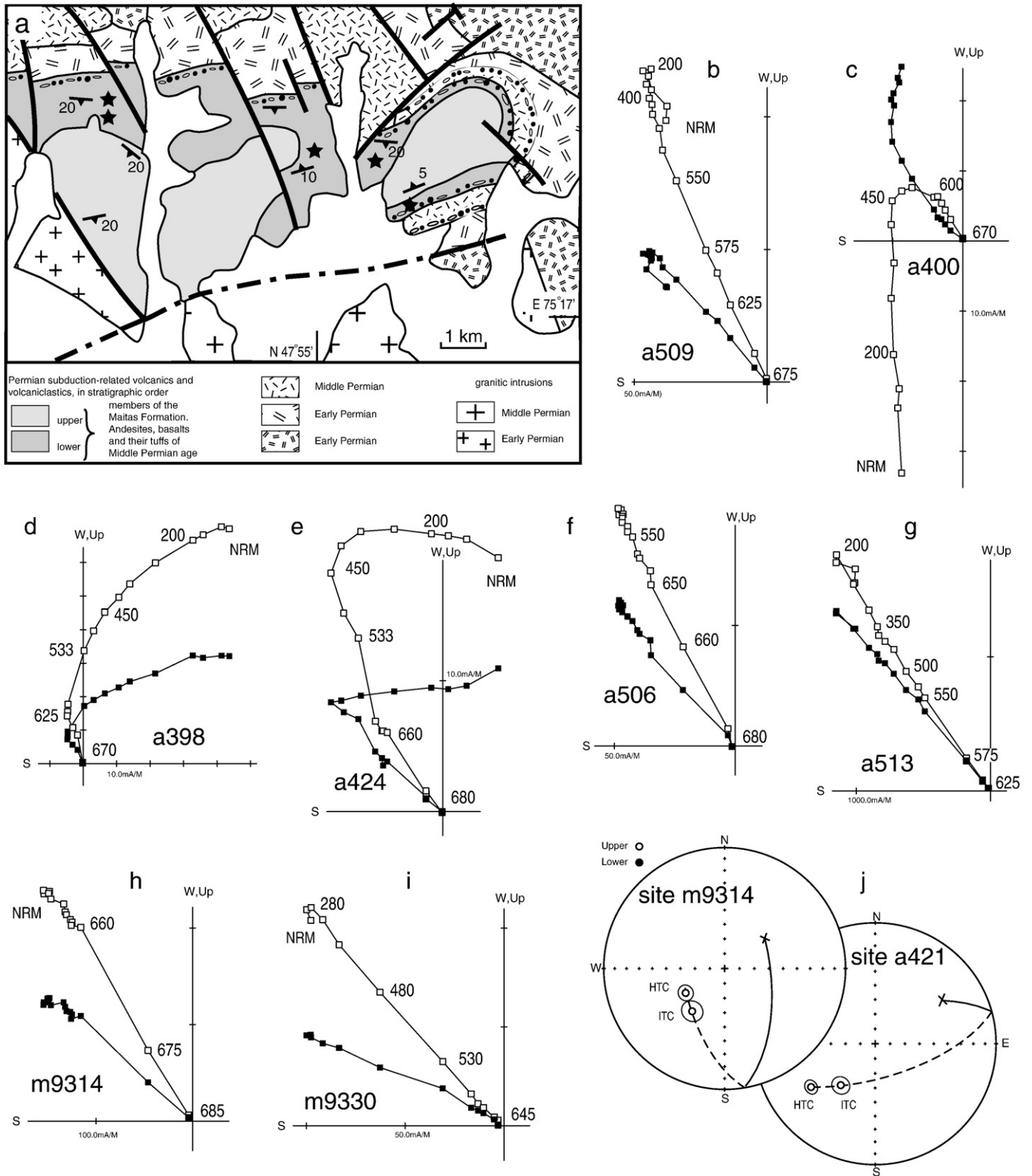


Fig. 3. (a) Geologic map of the Tokrau-B sampling locality. (b–i) Orthogonal demagnetization diagrams in tilt-corrected coordinates for representative samples of the Tokrau-B collection; conventions as in Fig. 2. (j) Examples of angular separation between site-mean magnetizations defined by “hematite” (labeled HTC) and “magnetite” (ITC) unblocking temperature ranges. Great circles fitted through HTC and ITC site-mean directions bypass the present-day field (PDF) direction, indicating that the ITC is not a composite HTC+PDF direction, but likely represents a meaningful ancient magnetization component.

Unlike any other continental interior, the central part of Kazakhstan displays a horseshoe-shaped belt with arc-volcanics of Devonian through Early Permian ages (Fig. 1), which unconformably overlie

older structures. The area internal to the strongly curved volcanic structures is dominated by rocks indicative of deeper marine environments, whereas the regions surrounding it were either non-depositional

highlands or epicontinental shallow-marine and non-marine basins (Zonenshain et al., 1990). The outer volcanic belt consists of a sequence of Upper Silurian to Middle Devonian extrusives. In the Frasnian, volcanic activity shifted to the more interior belt, ~150 km to the south, and continued there in the Famennian–Tournaisian. Further inward displacement of volcanic activity occurred in the Early Carboniferous and lasted until the Middle Permian (Tectonics of Kazakhstan, 1982). The composition of the volcanics, their calc-alkaline affinity and general progression from basalt to andesite and/or dacite and then to rhyolite in all belts, indicates that volcanics are subduction-related, and represent an Andean-type volcanic arc (Zonenshain et al., 1990; Bakhtiev, 1987, Kurchavov, 1994; Skrinnik and Horst, 1995).

Previous paleomagnetic studies have demonstrated that in the Middle Devonian the volcanic arc demarcated the eastern margin of Kazakhstania; the arc was nearly straight and NW–SE trending

(Abrajevitch et al., 2007). Today, the shape of this Devonian volcanic belt can be approximated by three linear segments: north-eastern (NE), middle (NW) and south-western (SW). Devonian paleomagnetic directions in different arms of the orocline show that the SW arm has experienced only a small cumulative clockwise rotation (~20°) after the Middle Devonian, whereas the middle arm has rotated clockwise by ~110°, and the NE arm by ~160° (Abrajevitch et al., 2007; Levashova et al., in press). The rotations are thought to have been largely completed by the Early Triassic (Van der Voo, 2004; Van der Voo et al., 2006); thus, the timing of the oroclinal orogeny can be considered as confined to the interval 385 Ma to 240 Ma. To characterize the final stages of the bending, and to better constrain its age, we have studied a set of Upper Carboniferous to Upper Permian rocks at two localities from the middle (locality Tokrau) and NE (locality Ayaguz) arms of the curved structure (Fig. 1).

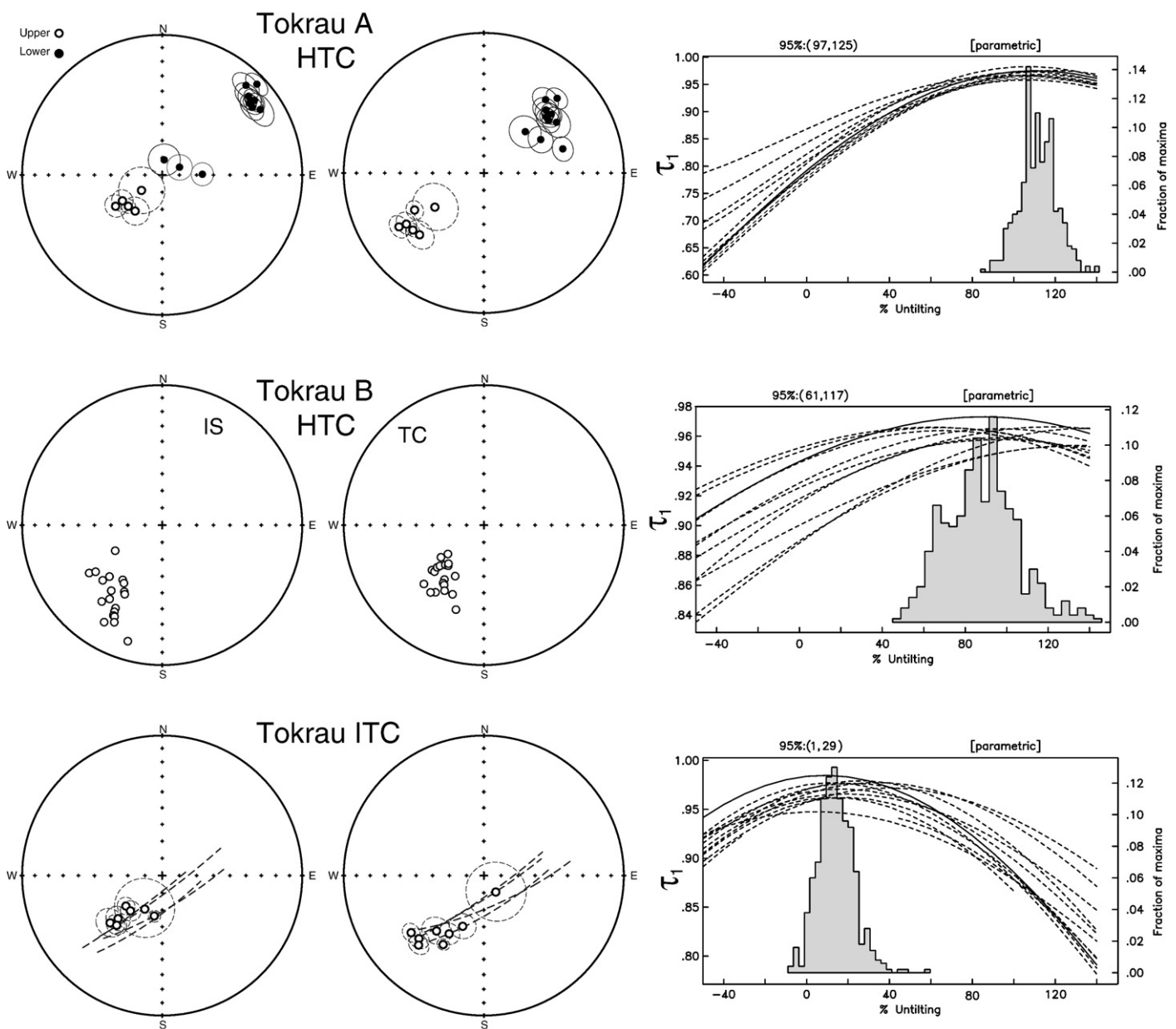


Fig. 4. Equal-area stereoplots of site-mean magnetization directions of the Tokrau localities (as also listed in Tables 1, 2 and 3); the left plots are *in situ* (IS), middle plots are in tilt-corrected (TC) coordinates. Open (closed) symbols represent upper (lower) hemisphere projections. The right column shows results of the parametric fold-tests (Tauxe and Watson, 1994) for the corresponding collections.

3. Sampling and laboratory methods

At all localities we sampled stratified rocks with various bedding attitudes to permit a fold test. Geological maps of the sampling areas and the locations of the sampling sites for individual collections are shown in Figs. 2a, 3a, 5a and 6a.

At both Tokrau and Ayaguz localities the sampled sections consist of lava flows and tuffs of dacitic to rhyolitic composition, ignimbrites, and volcanoclastic breccia with some conglomerates, sandstone and mudstone layers (Miasnikov, 1974). In the Ayaguz area, this sequence is called the Koldar Formation. In the Tokrau area, we studied the upper part of the Kalmakemel Formation, which is thought to be of Late Carboniferous–Early Permian age (Tevelev, 2001; Tevelev, pers. comm. 2005).

The middle member of the Koldar Formation at Ayaguz is characterized by a thick, laterally persistent sequence of lithoclastic tuffs with sedimentary interbeds. The age assignment for this formation is based on abundant flora (*Noeggerathopsis theodori* Zal. et Tschirk., *Phyllothea deliquescens* (Goepf.) Schm., *Paracalamites frigidus* Neub., etc.) found in the middle member (Miasnikov, 1974; Sal'menova and Koshkin, 1990), indicating deposition during the Kasimovian to mid-Kungurian stages, i.e., ~306 to 273 Ma (Gradstein et al., 2004; Menning et al., 2006).

At the Tokrau locality, in addition to the Kalmakemel Formation rocks, we sampled latest Early to Late Permian rocks of the Maitas Formation that overlies older formations with a dis- or un-conformity marked by a basal conglomerate (Fig. 3). The Maitas Formation consists of laterally varying volcanics of rhyolitic, andesitic and basaltic composition, associated tuffs and rare tuffaceous sediments. The age of the formation was determined based on lithologic–stratigraphic relationships and fossil flora content (*Paracalamites angustus* Such., *Noeggerathopsis concinna* Radcz. etc.) (Koshkin, 1974; Sal'menova and Koshkin, 1990) corresponding to the mid-Kungurian–Guadalupian–Lopingian (273–251 Ma) of the international geologic time scale (Gradstein et al., 2004).

Samples for this study were collected either as oriented blocks or with a gasoline-powered drill. Whenever weather permitted, both solar and magnetic compasses with an inclinometer were used for sample orientation. Both methods gave identical readings, indicating that magnetic intensities of the sampled rocks did not affect orientation measurements.

In the laboratory, standard specimens were prepared from the collected samples; cubes with ~20 mm side dimensions were cut from the block samples, and ~2.2 cm long cylinders from the 2.5 cm diameter drill cores. Measurements of natural remanent magnetization (NRM) were performed in a magnetically shielded room in the University of Michigan paleomagnetic laboratory using a three-axis 2G superconducting magnetometer. Alternating field demagnetization of a few pilot specimens failed to isolate components of magnetization successfully. The bulk of the specimens were therefore thermally demagnetized in an ASC TD-48 demagnetizer inside the shielded room with a residual field <200 nT. Results of the demagnetization treatments have been plotted in orthogonal vector endpoint diagrams (Zijderveld, 1967) and in stereonet. For calculation of the magnetization directions, principal component analysis (PCA, Kirschvink, 1980) was used on linear segments of the Zijderveld plots; in cases where stable endpoints were not obtained, as indicated by successive endpoints that could be seen moving as trends along great circle paths, a combined analysis of remagnetization circles and direct observations (McFadden and McElhinny, 1988) was used.

4. Results

4.1. Tokrau-A

Rocks of the Kalmakemel Formation sampled at Tokrau-A show consistent demagnetization behavior (Fig. 2). Apart from a viscous magnetization that is usually removed by 200–300 °C, all specimens

show a well defined (Maximum Angular Deviation (MAD) angle <3°) characteristic component which decays to the origin. The typical unblocking temperature range for this component is 550–675 °C, indicating hematite as the principal magnetization carrier, although in two sites (a464, m9382) ~80% of NRM intensity is lost between 533 and 566 °C, suggestive of fine-grained single-/pseudo-single domain (SD/PSD) magnetite as the main carrier of magnetization. Site-mean directions of the characteristic high temperature component pass the fold test (Fig. 4a; Table 1) as well as the reversal test of McFadden and McElhinny (1990) with observed $\gamma=3.11$ being smaller than the critical $\gamma=9.26$, strongly suggesting a pre-folding age of the magnetization.

In addition to the high temperature component, most of the samples reveal the presence of a second magnetization in the ~300–550 °C range. Some demagnetization diagrams show clear separation of the two components (e.g. Fig. 2h, i). For the others, the separation is incomplete due the overlapping temperature spectra of the high temperature (HTC) and the intermediate temperature component (ITC) components, and the ITC is revealed as a curved segment, or a kink (Fig. 2f, j). Wherever the curved segments were long enough, great circles were calculated for these segments. In sites that had both direct observation of the ITC and the great circles, the McFadden and McElhinny (1988) technique was used to calculate the site-mean direction of the ITC. When only the great circles were available, a site-mean great circle was calculated. The site-mean directions of the ITC show better grouping *in situ* (Fig. 4c; Table 2), indicating a post-folding age of this magnetization.

4.2. Tokrau-B

The Upper Permian rocks sampled at Tokrau-B show variable demagnetization behavior. In all specimens a low temperature component whose *in situ* direction is commonly (but not always) close to the present-day field (PDF) direction at Tokrau is usually removed by ~200–300 °C, although it occasionally persisted up to 550 °C (Fig. 3c). After removal of the low temperature component (LTC), sample magnetizations either show univectorial decay to the origin over the entire temperature range [300 °C–675 °C] or they have a change in direction between the magnetite [300–580 °C] and hematite [580–675 °C]

Table 1
High temperature component, Tokrau-A

Site	N	Bedding	In situ			Tilt-corrected		
			D	I	k	α_{95}	D	I
m9392	6/6	327/28	65.7	79.0	82.9	7.4	59.6	51.1
m9398	5/6	327/28	15.1	80.7	46.0	11.4	46.3	54.6
m9350	5/6	327/28	92.3	68.0	206.5	5.3	74.1	42.5
m9356	5/6	327/28	218.0	-65.9	83.9	8.4	227.2	-38.7
m9362	5/6	327/28	226.1	-75.0	33.1	13.5	227.7	-55.0
m9368	6/6	319/20	247.6	-71.1	160.7	5.3	241.7	-43.3
m9374	5/6	327/28	237.0	-62.3	148.4	6.3	237.0	-34.3
m9380	6/6	327/28	237.8	-57.1	124.0	6.0	237.5	-29.1
m9386	6/6	327/28	226.5	-63.0	296.0	3.9	231.2	-35.3
a430	7/7	152/20	52.6	21.7	265.1	3.7	50.3	41.4
a437	6/6	152/20	52.0	21.2	89.0	7.1	49.8	40.8
a452	6/6	152/20	47.6	17.8	82.3	7.4	44.7	37.1
a458	5/5	152/20	50.4	22.4	26.7	15.1	47.5	41.9
a464	6/6	152/20	46.3	4.1	302.7	3.9	44.9	23.3
a470	5/6	152/20	45.0	15.7	83.4	7.7	42.0	34.7
a476	6/6	152/20	53.5	17.0	44.9	9.3	51.8	36.7
a482	6/6	152/20	51.4	19.7	44.7	10.1	49.1	39.3
a488	6/6	152/20	48.9	19.4	367.2	3.5	46.1	38.8
Mean IS	18		51.3	43.7	8.4	12.7		
Mean TC	18				66.5	4.3	51.5	40.0

Legend and explanation for this table: Bedding measurements are given as the strike and dip angle (down dip to the right (clockwise) of strike). N indicates the ratio of samples studied/used in the statistical analysis. Dec and Inc are the declination and inclination of the site-mean direction (in °); α_{95} is the radius of the 95% confidence cone about the mean direction (in °); k is Fisher's (1953) concentration parameter. IS – *in situ*, TC – tilt-corrected directions.

Table 2
Intermediate temperature component, Tokrau

Site	N	Bedding	<i>In situ</i>			Tilt-corrected		
			D	I	k	α_{95}	D	I
m9314	3/6	238/11	217.2	-53.4	305.4	7.1	211.2	-49.5
m9326	4/6	238/11	232.6	-49.4	42.0	14.3	220.4	-47.2
m9356	2/6	327/28	209.8	-60.8	32.9		221.3	-34.5
m9368	6/6	319/20	227.7	-62.1	173.5	5.1	231.7	-34.3
m9374	5/6	327/28	212.8	-59.0	187.6	5.6	222.5	-32.4
m9380	5/6	327/28	219.8	-61.9	167.6	5.9	227.3	-34.6
m9386	6/6	327/28	189.3	-65.0	367.2	3.5	212.2	-41.8
a421	6/6	190/16	223.1	-50.3	172.0	5.9	203.5	-58.6
a430	3GCs	152/20	323.0	-9.2			326.7	-11.7
a458	3GCs	152/20	321.0	-7.1			324.1	-10.4
a476	2GCs	152/20	320.2	-17.3			327.0	-20.3
a482	3GCs	152/20	328.0	-18.0			336.0	-18.2
a488	6/6	152/20	208.6	-68.3	21.7	17.3	144.2	-78.1
Mean IS			216.0	-59.0	85.6	4.6		
Mean TC					23.2	8.8	218.9	-46.8

GCs – indicates that the corresponding directions listed are site-mean directions representing the poles to great circles rather than declinations and inclinations. Other notations are as in Table 1.

unblocking temperature ranges (Fig. 3e, h, i). This directional change could be explained by two different magnetizations in the corresponding unblocking temperature ranges, or by the incomplete removal of a low-temperature overprint in the magnetite range. Great circles fitted through the “hematite” and “magnetite” mean directions for each of these three sites bypass the present-day field direction (Fig. 3j), indicating that a magnetization in the “magnetite” temperature range is unlikely to be contaminated by a PDF-overprint, and it probably represents the true component of magnetization. The *in situ* directions and unblocking temperature range of this “magnetite” magnetization are similar to that of the ITC of the Tokrau-A collection, so the ITCs of these two collections were combined.

The highest temperature component that decays to the origin was designated as the characteristic remanent magnetization (ChRM; Table 3) component in the studied rocks. In two sites, the site-mean directions of the ChRM were found to be anomalous. In these anomalous

Table 3
High temperature, Tokrau-B

Site	N	Bedding	<i>In situ</i>			Tilt-corrected		
			D	I	k	α_{95}	D	I
a391	5/6	98/18	209.0	-43.6	133.2	6.7	221.7	-58.6
a397	6/6	98/18	209.2	-44.6	73.7	7.9	222.6	-59.5
a403	6/6	98/18	213.5	-49.1	33.9	13.0	231.8	-63.4
<i>a409</i>	6/6	98/18	<i>143.1</i>	<i>-60.2</i>	<i>155.7</i>	<i>5.4</i>	<i>109.9</i>	<i>-71.2</i>
a415	6/6	190/16	225.9	-46.6	262.5	4.1	209.4	-55.8
a421	6/6	190/16	237.1	-38.0	223.6	4.5	226.9	-50.1
m9314	6/6	238/11	241.9	-57.3	167.5	5.2	224.0	-57.7
m9320	4/6	238/11	227.4	-41.8	89.0	9.8	218.3	-38.9
m9326	6/6	238/11	235.1	-41.5	32.1	12.0	225.7	-40.0
m9332	6/6	238/11	215.2	-50.3	130.9	5.9	204.5	-45.1
a500	6/6	100/22	218.4	-31.1	78.7	7.6	228.9	-49.6
a506	5/5	100/22	218.1	-40.7	194.4	5.5	233.5	-58.8
a512	4/6	100/22	196.6	-15.0	82.1	10.2	198.3	-36.8
a518	4/5	100/22	210.7	-20.5	159.3	7.3	215.9	-40.8
<i>a524</i>	4/4	100/22	<i>242.8</i>	<i>-68.8</i>	<i>251.8</i>	<i>5.8</i>	<i>307.0</i>	<i>-71.1</i>
m9404	3/6	100/22	209.6	-32.8	77.5	14.1	228.0	-53.0
m9410	6/6	100/22	215.6	-35.8	10.4	21.8	227.4	-54.7
m9416	6/6	100/22	208.7	-28.0	66.1	8.3	215.3	-48.5
m9422	6/6	100/22	206.3	-24.1	35.5	11.4	211.2	-45.0
m9428	5/6	100/22	207.7	-27.3	19.4	16.7	213.8	-47.9
m9434	6/6	100/22	208.9	-30.1	90.0	7.1	216.1	-50.5
Mean IS	19/21		215.5	-37.4	31.8	6.0		
Mean TC	19/21				67.5	4.1	218.8	-50.6

Site-mean directions in italics (sites a409, a524) indicate that they are considered outliers, not to be used in the calculation of the collection-mean. Other notations as in Table 1.

Table 4
High temperature component, Ayaguz-A

Site	N	Bedding	<i>In situ</i>			Tilt-corrected		
			D	I	k	α_{95}	D	I
a1	4/4	116/25	261.7	-31.1	113.53	8.7	278.8	-42.2
a7	5/5	157/66	277.0	-1.8	169.29	5.9	304.1	-53.5
a14	3/4	156/65	266.7	4.2	108.39	11.9	283.4	-54.5
a18	4/4	156/65	272.9	1.0	128.31	8.1	294.9	-53.2
m7962	4/4	75/36	229.1	-60.4	38.78	14.9	292.1	-56.1
m7969	5/5	76/28	217.9	-56.7	49.7	13.2	268.2	-63.8
m7975	6/6	156/33	261.5	-30.3	37.6	10	274.6	-61.2
m7982	6/6	151/60	279.8	-7.7	32.9	11.9	307.5	-47.4
m7988	5/5	142/60	260.0	4.7	87.7	8.2	274.5	-46.1
p109	6/6	101/25	273.4	-40.9	64.2	8.8	295.0	-39.5
p120	4/4	85/27	239.9	-52.1	21.5	20.5	277.8	-55.2
p124	4/4	63/13	260.4	-54.3	107.7	8.9	275.4	-48.8
p128	4/4	11/20	270.5	-54.7	41.51	14.4	273.6	-34.9
p132	4/4	11/20	277.6	-47.6	44.12	14.0	278.4	-27.6
<i>t1</i>	4/4	111/15	<i>204.4</i>	<i>-72.5</i>	<i>5.5</i>	<i>43.0</i>	<i>223.5</i>	<i>-87.3</i>
<i>t7</i>	3/4	111/20	<i>266.6</i>	<i>-60.7</i>	<i>276.8</i>	<i>7.4</i>	<i>304.7</i>	<i>-62.7</i>
Mean IS	15		263.8	-33.9	8.1	14.3		
Mean TC	15				38.3	6.3	285.2	-50.5

Notations as in previous tables.

sites the directions of individual samples show a good clustering on the site level (lightning induced magnetization is unlikely), site-mean directions differ from the PDF (recent weathering is unlikely), the sites were sampled in monoclinical sections with good structural control (unrecognized structural complications are unlikely), but the site-mean anomalous directions differ significantly from the mean directions of the neighboring sites with similar bedding attitudes. These anomalous site-mean directions are listed in italics in Table 3 (denoting outliers), and they are not included in a calculation of the collection-mean. The ChRM directions of the remaining sites show better grouping upon tilt correction (Fig. 4b); a 95% confidence interval of the bootstrap fold test of Tauxe and Watson (1994), 61–117%, includes the 100% unfolding orientation, which indicates a pre-folding age of the magnetization.

4.3. Ayaguz-A

At Ayaguz-A, we sampled rocks of the Koldar Formation comprising tuffs of different grain-sizes and compositions and several volcanic flows. In addition, we sampled twenty clasts from an intraformational conglomerate for a conglomerate test. Studied rocks show variable demagnetization behavior that usually corresponds to the lithology. In volcanic flows, welded tuffs and ignimbrites, after the removal of a viscous component at ~250–300 °C, a single component of magnetization unblocks up to 675 °C. In coarser-grained tuff varieties the viscous magnetization usually persists to higher temperatures,

Table 5
High temperature component, Ayaguz-B

Site	N	Bedding	<i>In situ</i>			Tilt-corrected		
			D	I	k	α_{95}	D	I
a22	4/4	158/58	223.7	-52.4	141.8	7.7	101.6	-63.1
a30	4/5	115/44	217.6	-56.2	54.7	12.5	352.0	-77.1
a37	4/4	121/22	259.0	-52.8	142.3	7.7	291.3	-62.9
m7993	4/5	144/65	202.4	-50.2	205.0	6.4	89.8	-55.0
m7999	3/5	144/65	183.1	-57.6	16.9		87.7	-41.5
m8006	4/4	81/62	212.3	-50.8	316.8	5.2	308.9	-51.5
m8012	4/4	137/12	239.9	-33.5	56.3	12.4	242.3	-45.1
p136	3/2	161/16	227.9	-37.4	18.0		220.8	-51.7
p143	2/2	161/16	240.0	-50.3	872.9		233.7	-65.8
p149	5/5	116/15	265.4	-50.5	219.2	5.2	284.3	-56.0
p155	7/7	111/25	265.9	-50.6	369.2	3.1	299.2	-54.5
Mean IS	11		231.7	-51.9	21.0	10.2		
Mean TC	11				5.6	21.2	273.6	-80.1

Notations as in previous tables.

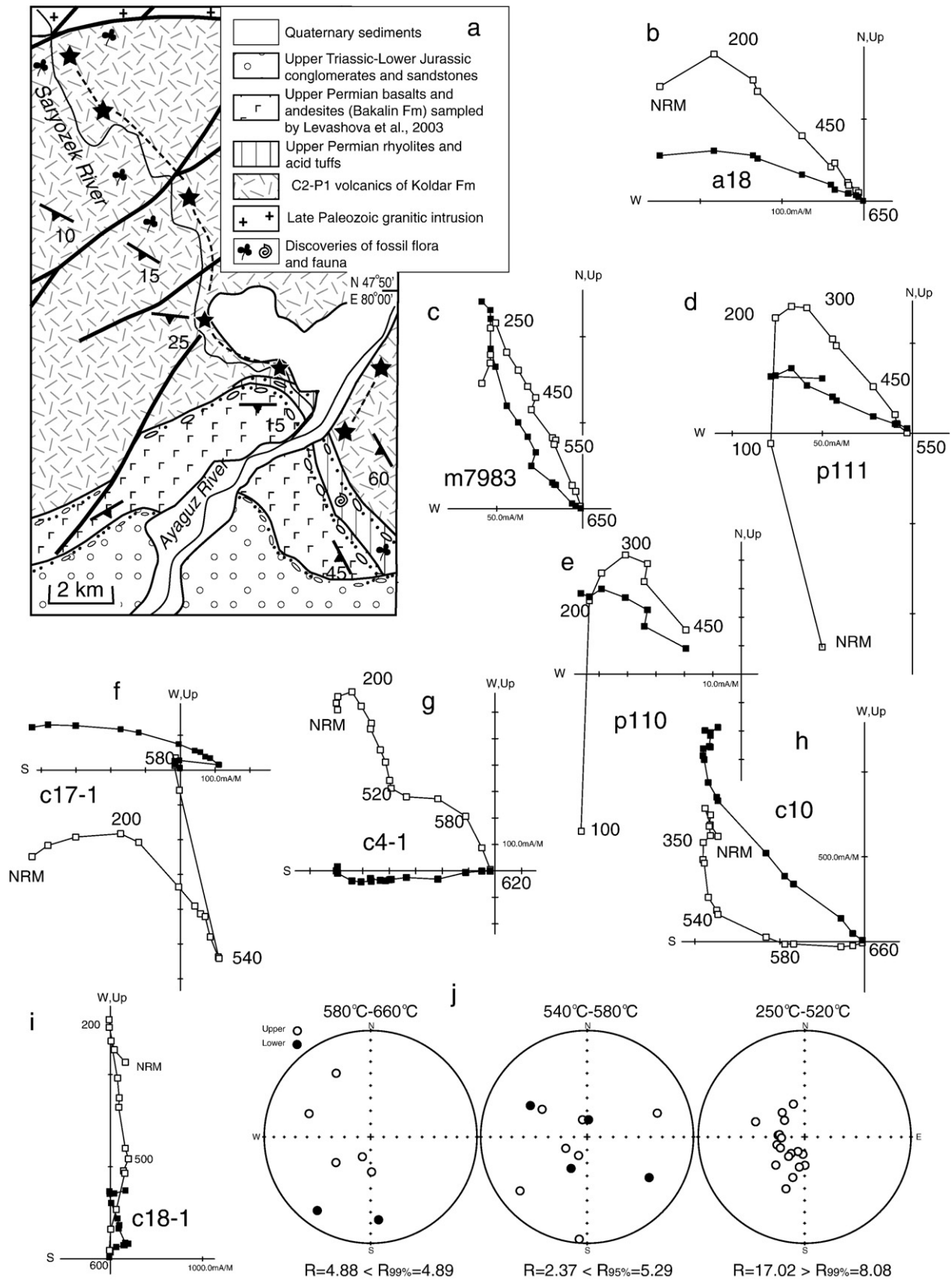


Fig. 5. (a) Geologic map of the Ayaguz-A sampling locality. (b–e) Orthogonal demagnetization diagrams in tilt-corrected coordinates for representative samples of the Ayaguz-A collection. (f–i) Examples of demagnetization diagrams (*in situ*) of conglomerate clasts. Plotting conventions for (b–i) as in Fig. 2. (j) Results of the randomness test for the clasts of an intraformational conglomerate. Plotting conventions as in Fig. 4. The low temperature (250–520 °C) component is not random, whereas randomness could not be disproved at 95% confidence level for the intermediate (540–580 °C) and at 99% confidence level for the high temperature (580–660 °C) components. Thus, the conglomerate test is positive for the two higher-temperature components.

sometimes displaying a strong overlap in the unblocking temperature range with the high temperature component. Nevertheless, in all sites it was possible to isolate the high temperature component showing a linear decay to the origin.

In one of the studied sites, the directions of the HTC are widely scattered ($\alpha_{95} > 43^\circ$); this site (t1) was excluded from further consideration and is listed in Table 4 in italics. The HTC of the remaining sites passes the fold test (Fig. 7), suggesting a pre-folding magnetization age.

Demagnetization behavior of the conglomerate clasts is generally different from that of the studied volcanics. Two specimens cut from the same clast (18 out of 20 studied clasts yielded two specimens) always show identical diagrams, but the behavior varies between the

clasts. After removal at $\sim 200^\circ\text{C}$ of the viscous magnetization whose direction is close to the PDF, the samples reveal two to three components of magnetization (Fig. 5f–i). Most of the samples display an upward pointing component unblocking between 250 and 520 $^\circ\text{C}$, and eleven samples show a change of trend in the 540–580 $^\circ\text{C}$ temperature range (e.g. Fig. 5f–g). The presence of magnetization components in the hematite temperature range [580–660 $^\circ\text{C}$] is evident in many samples (Fig. 5f–h), but only in seven samples could their directions be calculated with an acceptable precision, (e.g., $\text{MAD} \leq 10^\circ$ for a trajectory defined by at least 3 steps). To test for randomness (Watson, 1956), the components have been separated into three groups according to their unblocking temperature ranges. The low temperature component [250–520 $^\circ\text{C}$] fails the randomness

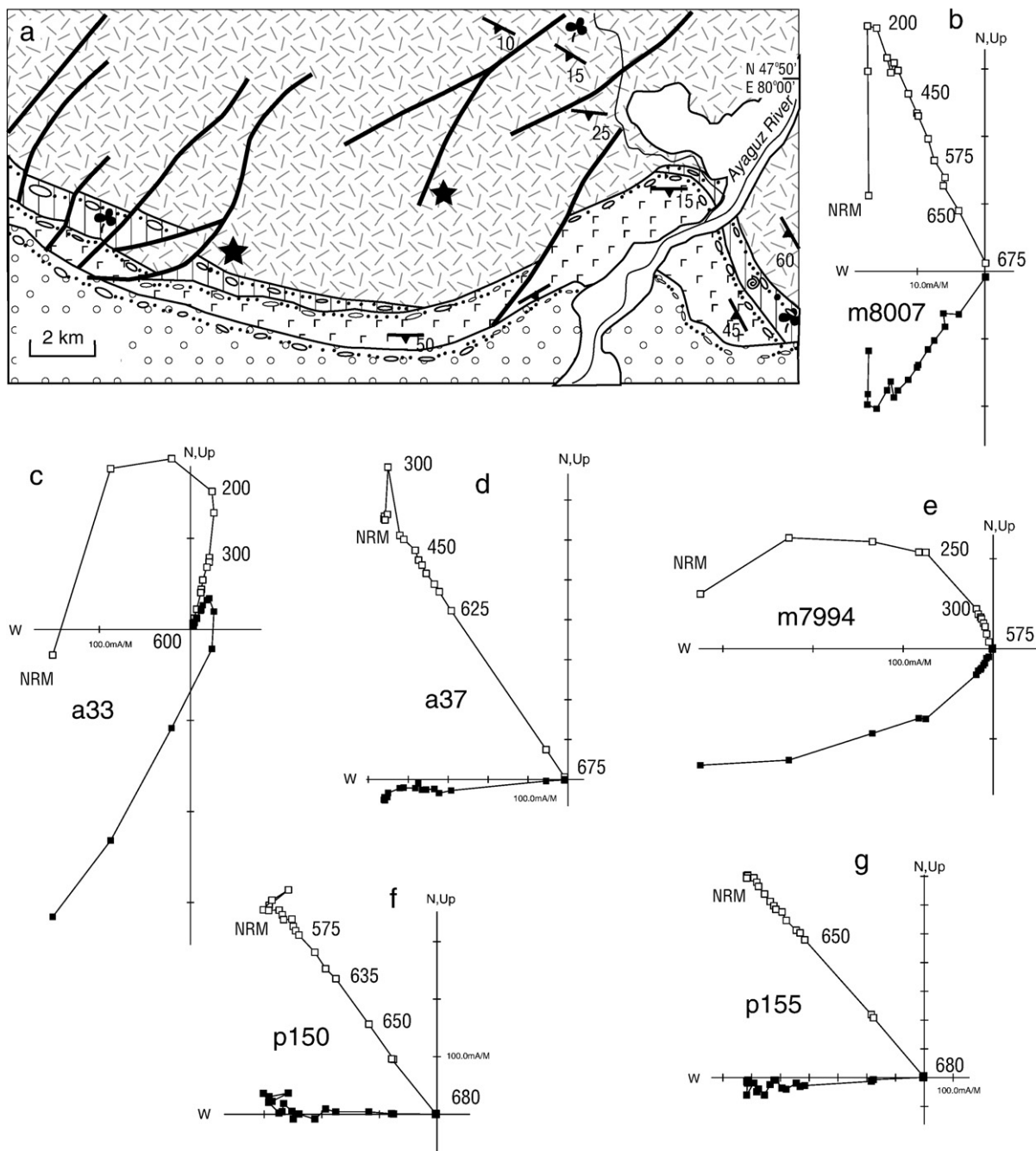


Fig. 6. (a) Geologic map of the Ayaguz-B sampling locality, for legend refer to Fig. 5a; stars represent sampling localities with multiple sites, which have varying bedding attitudes as listed in Table 4. (b–g) Orthogonal demagnetization diagrams (Zijderveld, 1967) in *in situ* coordinates for representative samples of the Ayaguz-B collection. Plotting conventions as in Fig. 2.

test; for the high temperature component [580–660 °C], the randomness cannot be disproved at 99% confidence level; and the intermediate temperature component [540–580 °C] is considered random at 95% confidence level. The co-occurrence of multiple magnetization components with different clustering indicates that although studied clasts did acquire a secondary magnetization during or after the conglomerate formation, remagnetization was limited to the temperature range below 520 °C. The positive conglomerate test for the higher-temperature components suggests that the clasts, and hence the studied volcanic rocks, in the area retained an ancient magnetization as characterized by unblocking >520 °C.

4.4. Ayaguz-B

The Koldar Formation rocks sampled at this locality show consistent demagnetization behavior. After the removal by ~200–300 °C of a viscous overprint whose *in situ* direction is similar to the PDF, most of the samples reveal a single magnetization component decaying to the origin (Fig. 6b–g). The bootstrap fold test of Tauxe and Watson (1994) applied to the site-mean directions of this magnetization (Fig. 7) shows that the best grouping is achieved between –34 and 14% unfolding, indicating a post-folding age of the magnetization.

5. Ages of magnetization

So far, in the studied collections, the age of magnetization has been determined relative to the folding, either as pre- or post-folding (see Table 6). The age of the folding itself, however, is often imprecisely defined, given that for both our sampling regions the deformation age is loosely described as “late Paleozoic” or “partly of early Mesozoic age” by, e.g., Sal'menova and Koshkin (1990) or Tevelev (2001). In such cases the

magnetization age may be additionally constrained by a comparison of the observed magnetization direction with reference directions that are predicted for the sampling area for a given time interval (Irving, 1964; Van der Voo, 1993). An internal reference frame for Kazakhstan is difficult to construct; large-scale deformations and shear-related block-rotations cause deviations in paleomagnetic declinations, resulting in an inconsistent apparent polar wander path (APWP). For the late Paleozoic, however, an external reference frame can be used. As argued by Puchkov (2002) and Levashova et al. (2007), Baltica and Kazakhstan were not far away from each other in the late Carboniferous, and were certainly welded by the Late Permian (Zonenshain et al., 1990; Natal'in and Şengör, 2005). Thus, the paleolatitudes of our study area should be in general agreement with those predicted by extrapolation from Baltica, and the degree of conformity should increase towards the Late Permian as the intervening Uralian Ocean progressively disappeared. A good agreement of late Paleozoic paleolatitudes for Kazakhstan with those predicted from Baltica paleopoles has previously been demonstrated (Van der Voo et al., 2006). Thus, in this study we use the global APWP of Torsvik et al. (in press) in Baltica's coordinates as a reference.

5.1. Tokrau

The rocks sampled at the Tokrau locality yielded three magnetization directions (Fig. 4): 1) a dual polarity pre-folding component, isolated in the Upper Carboniferous–Lower Permian rocks of the Tokrau-A collection; 2) an upward pointing pre-folding magnetization, observed in the Upper Permian rocks of the Tokrau-B collection; and 3) a post-folding magnetization, in both the Tokrau-A and B collections. The results are summarized in Table 6.

The positive fold test and especially the presence of reversals in the Tokrau-A rocks suggest (but do not prove) that the magnetization is

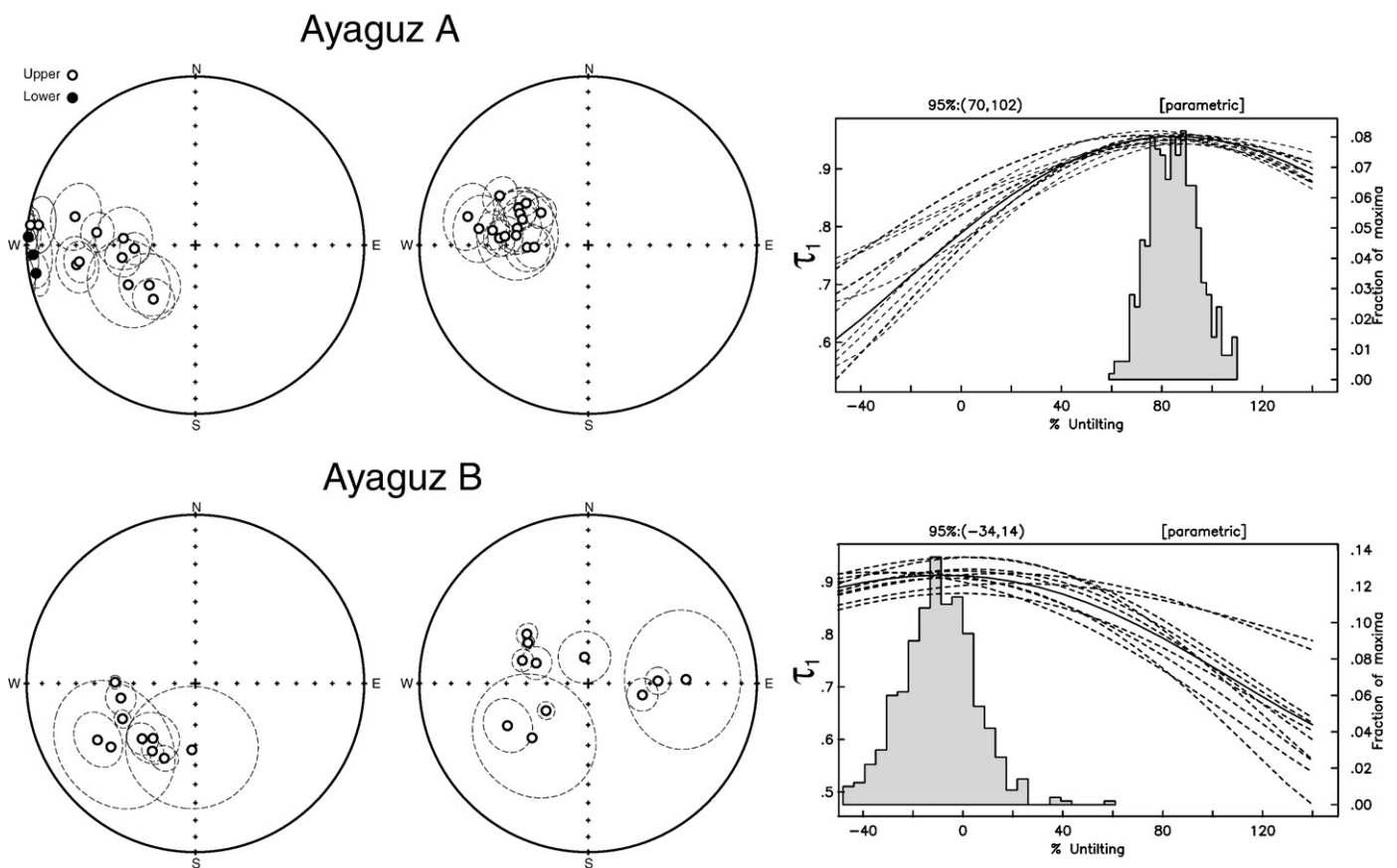


Fig. 7. Equal-area stereoplots of site-mean magnetization directions of the Ayaguz locality (as also listed in Tables 4 and 5); the left plots are *in situ*, middle plots are in tilt-corrected coordinates. The right column shows results of the parametric fold-tests for the corresponding collections. Other plotting conventions as in Fig. 4.

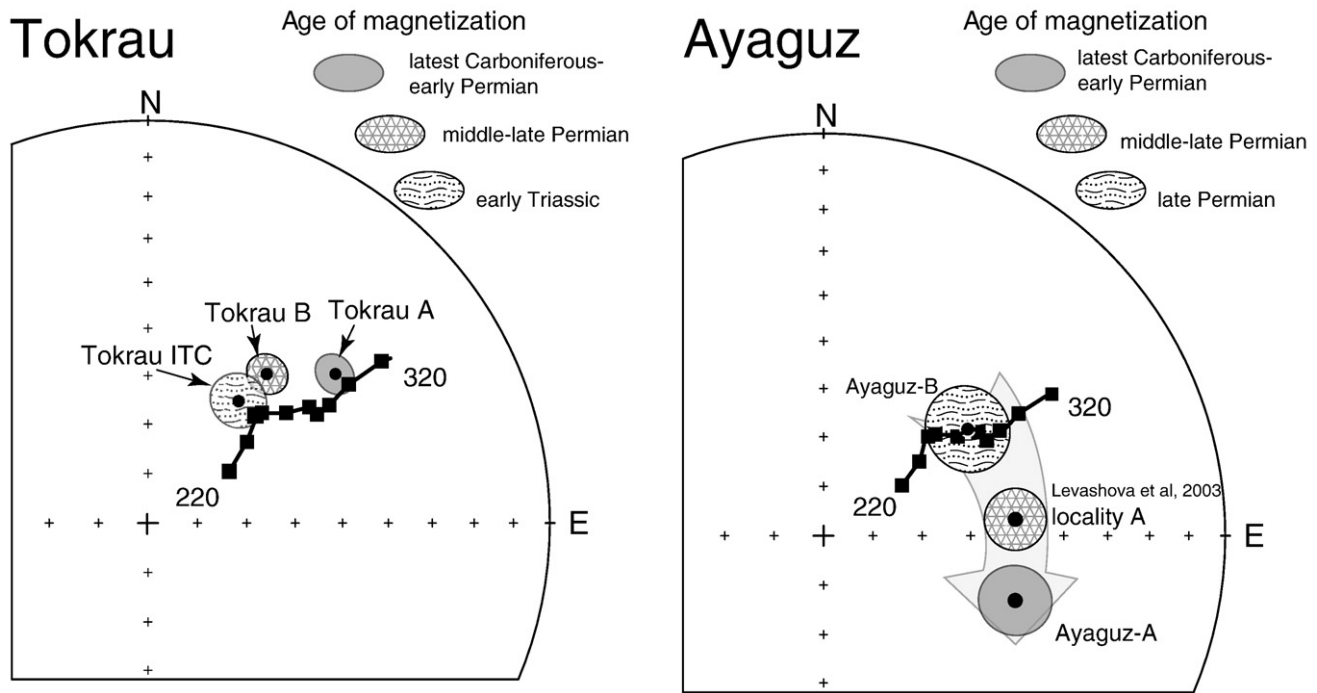


Fig. 9. Reference directions extrapolated from Baltica (black squares, plotted in 10 m.y. intervals, confidence limits are omitted for clarity) and directions of magnetization of the studied rocks. Filled circles are the mean magnetization direction, concentric ovals are cones of 95% confidence, and different shading signatures represent the inferred ages of magnetization. All directions are in the lower hemisphere, corresponding to normal-polarity field directions. The magnetization directions and their confidence circles from the Tokrau locality (middle arm of the orocline) overlap the error margins (not shown) of the coeval Baltica reference directions, indicating that rotations with respect to Baltica are not significant. In Ayaguz (north-eastern limb of the orocline), the distribution of the latest Carboniferous–Early Permian magnetization (Ayaguz-A, this study), middle–Late Permian (Locality-A of Levashova et al., 2003) and the Late Permian (this study; Ayaguz-B) magnetizations indicates progressive clockwise rotation of the study area with respect to Baltica, with a clockwise rotation of ~50° occurring between the latest Carboniferous and the Late Permian.

determination of the net tectonic rotation after magnetization acquisition. In further discussion we consider the dual polarity pre-folding component isolated in the Kalmakemel Formation at Tokrau-A as a primary magnetization of latest Carboniferous–Early Permian age, and use the ~300 Ma reference direction for the rotation estimate.

The pre-folding magnetization isolated in the Tokrau-B rocks is likely to be primary, dating to the time of the rock formation. Its inclination is shallower than that of the overprint (i.e. it is older than Early Triassic), but steeper than that of the Tokrau-A rocks (i.e. it is younger than Early Permian), and agrees well with the reference inclination for the Late Permian (stratigraphic) age of the rocks.

5.2. Ayaguz

The Ayaguz sampling locality yielded two magnetization components (Fig. 7; Table 6): 1) a pre-folding upward pointing magnetization isolated from the latest Carboniferous–Early Permian rocks at Ayaguz-A (Koldar Formation); and 2) a post-folding magnetization in the Ayaguz-B collection.

When corrected for tilt, the inclination of Ayaguz-A agrees well with the ~275–305 Ma age range deduced from the reference inclinations (Fig. 9), which is the same age as assigned to this formation based on its fossil content and stratigraphic relationships. This good agreement indicates that the magnetization dates to the formation of the rocks and therefore may be considered primary. As is in the case of Tokrau-A, a somewhat broader age range does not affect estimates of post-Early Permian rotations of the Ayaguz area because the reference declination does not change perceptibly during this period.

The negative fold test for Ayaguz-B indicates that this remanence is post-folding. The *in situ* inclination of this magnetization best fits the 280–270 Ma reference directions, and the radius of the 95% confidence cone (α_{95}) about the mean suggests that, at the 95% probability level, this magnetization was acquired before 250 Ma (Fig. 9). Consequently,

although the magnetization is secondary, we can nevertheless be reasonably confident that the remanence is Permian in age.

6. Discussion

6.1. Rotations

Fig. 9 shows the distribution of the observed magnetization components relative to the reference directions calculated by extrapolation from the APWP in Baltica coordinates (Torsvik et al., *in press*) for the two sampling localities. As this plot demonstrates, all three magnetization components isolated at the Tokrau locality are close to their coeval reference directions. A slight counterclockwise deflection of the observed directions could be explained by a post-Early Triassic

Table 6
Summary of paleomagnetic results

Result	Age	Tests	D	I	k	α_{95}	Plat	Plong	dp	dm
Tokrau-A	~305–275 Ma	F ⁺ R ⁺	51.5	40.0	66.5	4.3	42.2	178.8	5.2	3.1
Tokrau-B	275–251 Ma	F ⁺	218.8	-50.6	67.5	4.1	56.3	180.6	5.5	3.7
Tokrau-	early Tr	F ⁻	216.0	-59.0	85.6	4.6	63.1	169.6	6.9	5.1
overprint										
Ayaguz-A	~305–275 Ma	F ⁺ C ⁺	285.2	-50.5	38.3	6.3	13.5	138.0	8.5	5.7
Ayaguz-B	late P	F ⁻	231.7	-51.9	21.0	10.2	48.5	172.1	13.9	9.5

Age: for pre-folding and presumably primary magnetizations it is indicated as a stratigraphic age of the sampled rocks according to the International stratigraphic scale (Menning et al., 2006); for post-folding magnetizations, the age is assigned based on a comparison with reference directions obtained by extrapolation from Baltica's APWP (Torsvik et al., *in press*).

Tests: F fold; R reversals; C conglomerate; superscripts: T⁻ indicates negative; T⁺ positive field test.

Directions and associated statistics are presented in stratigraphic coordinates for pre-folding magnetizations, and in geographic coordinates for post-folding remanence. Pole coordinates are given for the north poles.

rotation, but this deviation is statistically insignificant for the older Tokrau-A and the younger Tokrau-overprint (i.e., the error limit (ΔR) about the rotation estimate overlaps a zero rotation value). Therefore we can only conclude that, for all practical purposes, no significant rotations occurred between the Tokrau area (i.e. the middle limb of the orocline) and Baltica since the Early Permian. Apparently, the middle limb of the orocline was in the same orientation with respect to Baltica in the Early Permian as it is today; the bending of this part of the curved structure was over by that time.

The older magnetization component observed in the Ayaguz locality by our study and the late Early to Late Permian result (“L–A”) from the Bakalin Formation in the same area (see Fig. 5a) published by Levashova et al. (2003), have declinations that differ from those extrapolated from Baltica. The younger (~275–250 Ma) magnetization is deflected clockwise by $19.8 \pm 4.3^\circ$, and the older (~295–305 Ma) Ayaguz-A magnetization is deflected clockwise by $47.7 \pm 6.2^\circ$ (Fig. 9). On the other hand, the post-folding (likely Late Permian) declination of Ayaguz-B is statistically indistinguishable from the reference directions. The declination trend of the Ayaguz results (Fig. 9) suggests that since the latest Carboniferous–Early Permian (and very likely before the Early Triassic) the Ayaguz locality underwent a clockwise rotation of about 50° with respect to Baltica.

It is tempting to interpret this rotation as evidence for the last rotation phase of the bending of the entire NE arm of the orocline. However, we do not have sufficient coverage of Permian paleomagnetic results in the Chingiz Range of the NE limb. The limited number of reliable Permian data allows another possibility, involving localized shear-related block-rotations, just as was argued for the SW limb (Van der Voo et al., 2006; see also Wang et al., 2007). In either case, the progressive rotations observed in the Ayaguz results suggest that the NE arm was still undergoing active deformation during the Late Permian. Levashova et al. (2003) reached a similar conclusion based on the more limited results from the Bakalin Formation alone for this area.

Combining the constraints provided by our new data with those of our other recent studies (Levashova et al., 2007; Abrajevitch et al., 2007; Levashova et al., in press), we can reconstruct a scenario of oroclinal bending in Kazakhstan. Table 7 lists the Devonian declinations. These paleomagnetic data strongly support oroclinal bending, because the structural trends of the limbs of the orocline (see also Fig. 1) correlate well with measured rotations (Abrajevitch et al., 2007; Levashova et al., in press).

Deformation continued after the oroclinal bending was nearly completed into the Late Permian–Early Triassic, causing localized rotations in the vicinity of strike-slip faults, as documented for the North Tien Shan by Van der Voo et al. (2006) and Wang et al. (2007). Late deformation can be interpreted within a framework of left-lateral

shear between Siberia and Baltica (Natal'in and Şengör, 2005). This means that in order to isolate the rotations due to orocline formation, one first has to restore the Devonian declinations of areas affected by these localized rotations, as has been done by Abrajevitch et al. (2007).

Using Baltica's Late Permian paleopole as a reference, we plot the structural trends with respect to the Late Permian meridian (when oroclinal bending had terminated). The required corrections to the present-day trends range from 44 to 48° for Kazakhstan's orocline. The resulting corrected orientations are listed in Table 7, and are used to position the orocline at the end of the Paleozoic in Fig. 10. Ideally, it would be useful in Table 7 to provide not just the declination and strike or orientation values that we have calculated, but also their error limits. However, for most of the information, listing any error ranges would be imprecise at best and unsubstantiated at worst.

6.2. Geodynamic implications

The sequence of deformations that we can deduce from the middle to late Paleozoic paleomagnetic results suggests that the mechanism that produced the strong curvature was bending of Kazakhstan in response to compressive stresses exerted by the convergence of neighboring continents. The varying magnitude of the relative oroclinal rotations along the arc with respect to the Late Permian meridian, from small in the SW arm ($\sim 25^\circ$ counterclockwise) to large in the NE arm ($\sim 120^\circ$ clockwise, Table 7), suggests that a dextral shear and drag was applied to the northern end of the structure, while its southern end was pinned by a backstop. This conceptual model, based on paleomagnetic declination and paleolatitude data, can also be tested with geological evidence.

The backstop at the southern end of Kazakhstan was likely created by its collision with Tarim. The initiation of the collision between Kazakhstan and Tarim in the Late Devonian is documented by deformations and emplacement of granite in the Central Tien Shan (Cai et al., 1996), by an inferred change in Tarim's motion (Chen et al., 1999), and by extensive Late Devonian rifting in Kazakhstan (e.g. Veimarn and Milanovsky, 1990; Bykadorov et al., 2003), as such rifting is commonly associated with a switch in tectonic mode following an accretion event (Lister et al., 2001).

The most likely candidate for imposing a shear stress on the northern end of Kazakhstan is the Siberian craton. Although the late Paleozoic APWP for Siberia is poorly constrained (e.g., Cocks and Torsvik, 2007), reliable paleomagnetic poles for 360 and 250 Ma have been reported by Kravchinsky et al. (2002) and Pavlov et al. (2007). The difference in the pole positions indicates that Siberia underwent a significant clockwise rotation in this Permo-Carboniferous time interval. It is plausible that the Carboniferous movements of Siberia also had a dextral shear component with respect to Kazakhstan and

Table 7
Rotation angles deduced for the Devonian results from the three limbs of the Kazakhstan orocline

Locality or formation	Best age estimate	Decl.	Approximate strike of Devonian arc today	Declination w.r.t. Late Permian Meridian	Approximate strike of Devonian Arc in the Permian	Reference
Northeast limb (48N, 80E)			120		72	
Kurbakanas (KU-L2)	392–385 Ma	167		119		Levashova et al. (in press)
G1	416–385 Ma	168		120		Grishin et al. (1997)
Kaynar-Dogolan	407–397 Ma	148		100		Levashova et al. (in press)
Northwest (middle) limb (48N, 76E)			70		24	
G2	416–385 Ma	111		65		Grishin et al. (1997)
Southwest (NTS) limb (44N, 76E)			–55		–99	
Kurgasholak	398–385 Ma	27*		–17		Abrajevitch et al. (2007)
Aral (L1)	385–359 Ma	16*		–28		Levashova et al. (2007)
Redbeds K1	416–398 Ma	23*		–21		Klishevich and Kramov (1993)
K2	416–392 Ma	22*		–22		Klishevich and Kramov (1993)

* mean declinations corrected for Permian-Triassic shear-zone related rotations (see Abrajevitch et al., 2007).

Orientation angles and strikes are positive (negative) when striking east (west) of north.

The arc's strike today (-55°) and the Devonian declination in the SW limb of about 20° , means that in the Devonian the arc in the Tien Shan area was striking about -75° . In the Permian, the declination was about 45° , yielding a strike of about -100° at that time (see Fig. 10). The cumulative post-Devonian rotation of this SW limb of $\sim 20^\circ$ clockwise with respect to the meridians consists therefore of a 25° counterclockwise rotation during the late Paleozoic, followed by a 45° clockwise rotation after the Paleozoic.

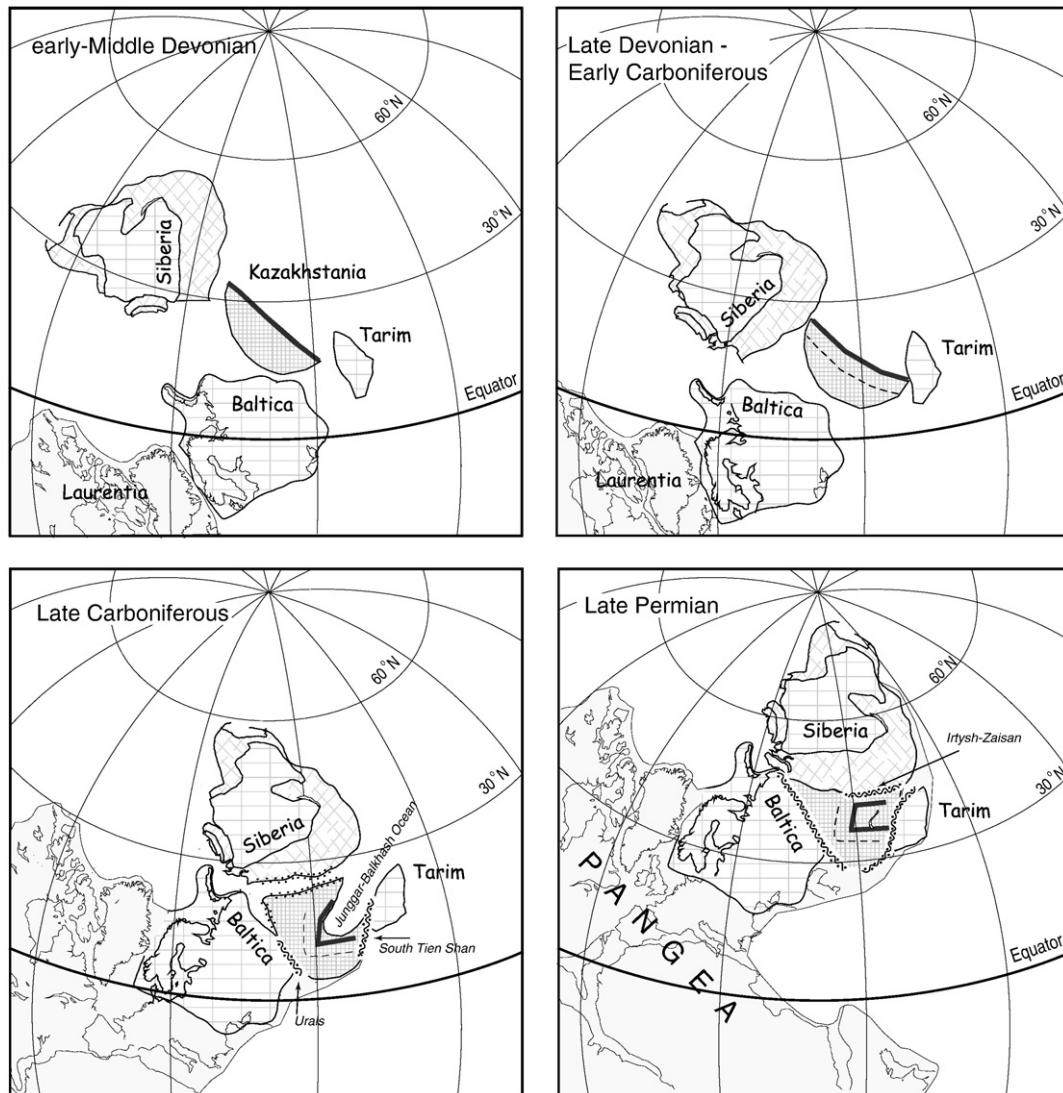


Fig. 10. Tectonic scenario for the bending of the Kazakhstan orocline. In the Late Devonian, Tarim and Kazakhstania collided, pinning Kazakhstania's southern corner. Dextral shearing and considerable clockwise rotation of Siberia resulted in Kazakhstania's northern end being dragged clockwise with respect to its relatively fixed southern end. Carboniferous continued convergence between Siberia and Tarim enhanced the buckling of Kazakhstania, trapped between them, leading to a subdivision of the belt into its three more or less orthogonal segments. The intervening Junggar-Balkhash Ocean was closed by Late Permian times after dual (divergent) subduction at opposite limbs of the tightening orocline. Reconstructions are based on APWP data in Baltica's coordinates (Torsvik et al., in press), Siberia's paleopoles (Kravchinsky et al., 2002; Pavlov et al., 2007), and Tarim's results (data averaged from the listing of Van der Voo, 1993 and those of Chen et al., 1999). The solid line denotes the Devonian Volcanic Belt above the pre-Late Permian subduction zone of the Junggar-Balkhash ocean basin.

Baltica (Fig. 10), although this latitude-parallel motion cannot be estimated from paleomagnetic data alone. However, paleogeographic reconstructions for the Late Devonian (e.g. Kravchinsky et al., 2002), indicate that Siberia's then-southern (now-western) margin was located at $\sim 20\text{--}30^\circ\text{N}$, similar to the paleolatitude of the northern tip of Kazakhstania (Grishin et al., 1997; Abrajevitch et al., 2007; Levashova et al., in press). The lateral displacement of Siberia between the Late Devonian and Permian may, therefore, have been accommodated by dextral shear along Kazakhstania's then-northern margin. Siberia's lateral displacement, accompanied by relative convergence of Siberia and Tarim, caused the Carboniferous buckling of the Kazakhstania microcontinent trapped between them.

To accommodate such large-scale oroclinal bending, crustal material must either be significantly shortened or be removed from between the converging arms. In the case of the Kazakhstan orocline, the crust of the Junggar-Balkhash Ocean between the converging arms was consumed at the surrounding subduction zones (Fig. 10). Because subduction-related Carboniferous and Early Permian volcanics are found on both SW and NE limbs of the orocline (Fig. 1),

subduction is likely to have occurred in a divergent pattern away from the then-oceanic center of the tightening orocline. An approximate estimate for the average subduction velocity is based on the width (~ 1200 km) of the oceanic crust that must have been consumed in the concurrent subduction zones in the time interval between the Late Devonian and Late Permian ($\sim 360\text{--}260$ Ma); this yields a geologically reasonable, even modest, value of ~ 6 mm/yr per subduction zone.

The buckling of the volcanic arc should also produce a specific deformation pattern, with contractional features along the inside of the developing orocline and extension on the outside, with maximum contraction expected within the inside of the hinges. In full agreement with these predictions, the hinge areas of the Devonian volcanic belt show evidence for significant contraction. In the northern part of the Spassk anticlinorium (a hinge zone between the middle (NW) and NE arms, labeled Sa in Fig. 1) isoclinal flow folds and strike-slip faults form "squeeze-out" structures that date to the early-middle Carboniferous (Suvorov, 1963; Chitalin, 1983). In a hinge zone between the SW and middle arms of the orocline, i.e., in the ~ 150 km wide Sarysu-Tengiz uplift (labeled ST in Fig. 1), the compression produced a system of

closely spaced subparallel reverse faults that accommodated some 150–200 km of shortening (Tikhomirov, 1975; Zonenshain et al., 1990).

While compressional deformations dominated the inner arcs of the hinge zones of the volcanic belt, the areas external to the oroclinal bend saw the development of large sedimentary basins. Late Devonian–Permian sequences consisting of intercalated continental clastics and shallow-marine deposits, have a thickness of over 6 km in the Chu–Sarysu Basin and over 7.5 km in the Tengiz Basin (Yakubchuk, 1997); these large thicknesses suggest that syn-depositional creation of an accommodation space for these sediments was likely driven by extension and subsidence.

All in all, the available paleomagnetic and geologic data are consistent with a model in which oroclinal bending of Kazakhstan's arc resulted from relative convergence between Siberia and Tarim, causing buckling and rotations of the arc's limbs (Fig. 10). Progressive large-scale bending of Kazakhstan was accompanied by continuous subduction-related magmatism and by gradual consumption of oceanic crust between the converging arms. The contemporaneous nature of these processes suggests that the belt of volcanic products was continuously being reoriented and tightened above the changing positions of the downgoing slabs. This, in turn, indicates that oroclinal bending was lithospheric in scale, with the basal plane (above which the rotations occurred) situated just above the subducting slabs in the upper mantle.

While such lithospheric bending has been proposed for some Alaskan terranes, the Olympic Mountains orocline in the State of Washington, and the Northland–Norfolk–New Caledonia–D'Entrecasteaux orocline near the Vanuatu–New Hebrides Arc of the southwest Pacific (Johnston, 2001; Johnston and Acton, 2003; Johnston, 2004), thus far there have been limited or no paleomagnetic data that can be listed as evidence for such an oroclinal process that involved much of the lithosphere. Thus, our recent and present studies may constitute some of the first paleomagnetic evidence for oroclinal bending involving the entire crust, rather than the much better known and well-documented oroclinal rotations in just the upper crustal setting above a décollement zone.

7. Conclusions

Our paleomagnetic study of latest Carboniferous to Late Permian rocks from the middle and north-eastern limbs of the Kazakhstan orocline has documented several magnetization directions. At the Tokrau sampling locality (within the middle arm of the orocline), three components of magnetization have been isolated: 1) a pre-folding dual polarity primary magnetization of latest Carboniferous–Early Permian age at Tokrau-A; 2) a pre-folding primary magnetization of the Late Permian age at Tokrau-B; and 3) an overprint likely of early Triassic age. The directions are statistically similar to their coeval reference directions obtained by the extrapolation from the global APWP in Baltica's coordinates. This correlation indicates that no significant rotations occurred between the middle limb of the orocline and Baltica since the latest Carboniferous–Early Permian and therefore, that the bending of this part of the curved structure was over by that time.

Two magnetization components have been isolated in the Ayaguz locality (within the NE limb of the orocline): 1) a pre-folding, likely primary magnetization of latest Carboniferous–Early Permian age at Ayaguz-A; and 2) a post-folding magnetization likely of Late Permian age at Ayaguz-B. These two directions differ in their position with respect to the reference directions. While the Late Permian magnetization of Ayaguz-B is statistically indistinguishable from both the coeval Tokrau-B magnetization and the reference direction, the latest Carboniferous–Early Permian Ayaguz-A magnetization is deflected clockwise by $47.7 \pm 6.2^\circ$. The deflection of this Ayaguz-A magnetization suggests that the studied area underwent a clockwise rotation of $\sim 50^\circ$ relative to Baltica during the Permian.

The estimates of these rotation angles, combined with the data on the Middle Devonian configuration of the belt (see Abrajevitch

et al., 2007) lead us to suggest the following scenario for the bending of the Kazakhstan orocline. A Late Devonian orogeny started when an initial collision occurred between Tarim and Kazakhstania (Fig. 10). This pinned Kazakhstania's southern corner, while a dextral shear motion and a considerable clockwise rotation of Siberia dragged its northern end, forcing it to buckle with respect to its southern end (the modern North Tien Shan). Relative convergence between Siberia and Tarim during the Carboniferous enhanced this buckling and led to the subdivision of the belt into the three segments recognizable in modern maps (Fig. 1). Continued subduction under the opposing arc-limbs eventually led to closure of the intervening Junggar–Balkhash Ocean, while tightening of the orocline continued. By the Late Permian the Junggar–Balkhash Ocean had ceased to exist.

Acknowledgements

We thank the reviewers of the journal, Stephen T. Johnston and Trond H. Torsvik for their valuable comments that improved the manuscript, and Chris Hall for his extensive help and advice with respect to the argon–argon dating results. We also thank many colleagues from the Scientific Station of the Russian Academy of Sciences in Bishkek (Kyrgyzstan) for logistic support of the fieldwork. This study was supported by the Division of Earth Sciences and the Office of International Science and Engineering's Eastern and Central Europe Program of the U.S. National Science Foundation, grant EAR 0335882. Support was also derived from the Russian Foundation of Basic Research, grants 04-05-64050 and 05-05-65105.

Appendix A. Supplementary data

Supplementary data associated with this article can be found, in the online version, at [doi:10.1016/j.tecto.2008.05.006](https://doi.org/10.1016/j.tecto.2008.05.006).

References

- Abrajevitch, A.V., Van der Voo, R., Levashova, N.M., Bazhenov, M.L., 2007. Paleomagnetism of the mid-Devonian Kurgasholok Formation, Southern Kazakhstan: constraints on the Devonian paleogeography and oroclinal bending of the Kazakhstan volcanic arc. *Tectonophysics* 441, 67–84.
- Bakhtiev, M.K., 1987. Paleozoic Orogenic Magmatic Belts. Nauka, Moscow. 168 pp. (In Russian).
- Bykadorov, V.A., Bush, V.A., Fedorenko, O.A., Filippova, I.B., Miletenko, N.V., Puchkov, V.N., Smirnov, A.V., Uzhkenov, B.S., Volozh, Y.A., 2003. Ordovician–Permian paleogeography of central Eurasia; development of Palaeozoic petroleum-bearing basins. *Journal of Petroleum Geology* 26, 325–350.
- Cai, D., Lu, H., Jia, D., Wu, S., Chen, C., 1996. $^{40}\text{Ar}/^{39}\text{Ar}$ dating of the ophiolite melange in the southern Tien Shan and the mylonite in the southern rim of central Tien Shan and their tectonic significance. *Dizhi Kexue = Scientia Geologica Sinica* 31, 384–390.
- Carey, S.W., 1955. The orocline concept in geotectonics, part I. *Papers and Proceedings of the Royal Society of Tasmania* 89, 255–288.
- Chen, C., Lu, H., Jia, D., Cai, D., Wu, S., 1999. Closing history of the southern Tianshan oceanic basin, western China; an oblique collisional orogeny. *Tectonophysics* 302, 23–40.
- Chitalin, A.F., 1983. The upper Paleozoic structure of the eastern part of the Spassk Anticlinorium and its frame (Central Kazakhstan). *Moscow University Geology Bulletin* 38 (4), 26–34.
- Cocks, L.R.M., Torsvik, T.H., 2007. Siberia, the wandering northern terrane, and its changing geography through the Palaeozoic. *Earth-Science Reviews* 82, 29–74.
- Cornell, R.M. and Schwertmann, U., 2003. The iron oxides. Structure, properties, reactions, occurrences and uses. Wiley-VCH Verlag GmbH & Co. KGaA, Weinheim, p. 664.
- Didenko, A.L., Mossakovsky, A.A., Pechersky, D.M., Ruzhentsev, S.V., Samygin, S.G., Kheraskova, T.N., 1994. Geodynamics of Paleozoic oceans of Central Asia. *Geology and Geophysics* 35, 118–145 (in Russian).
- Dobretsov, N.L., Berzin, N.A., Buslov, M.M., 1995. Opening and tectonic evolution of the Paleo-Asian ocean. *International Geology Review* 37, 335–360.
- Filippova, I.B., Bush, V.A., Didenko, A.N., 2001. Middle Paleozoic subduction belts: the leading factor in the formation of the Central Asian fold-and-thrust belt. *Russian Journal of Earth Sciences* 3 (6), 405–426.
- Fisher, R.A., 1953. Dispersion on a sphere. *Proceedings of the Royal Society of London. A* 217, 295–305.
- Gialanella, P.R., Heller, F., Haag, M., Nurgaliev, D., Borisov, A., Burov, B., Jasonov, P., Khasanov, D., Ibragimov, S., Zharkov, I., 1997. Late Permian magnetostratigraphy on the eastern Russian Platform. *Geologie en Mijnbouw* 76 (1–2), 145–154.
- Gradstein, D.M., Ogg, J.G., Smith, A.G., et al., 2004. *A Geologic Time Scale*. Cambridge University Press.

- Grishin, D.V., Pechersky, D.M., Degtyarev, K.E., 1997. Paleomagnetism and reconstruction of Middle Paleozoic structure of Central Kazakhstan. *Geotectonics* 1, 71–81.
- Hounslow, M.W., Davydov, V.I., Klootwijk, C.T., Turner, P., 2004. Magnetostratigraphy of the Carboniferous; a review and future prospects. *Newsletter on Carboniferous Stratigraphy* 22, 35–41.
- Irving, E., 1964. Paleomagnetism and Its Application to Geological and Geophysical Problems. John Wiley & Sons, New York, p. 399.
- Johnston, S.T., 2001. The Great Alaskan Terrane Wreck: reconciliation of paleomagnetic and geological data in the northern Cordillera. *Earth and Planetary Science Letters* 193, 259–272.
- Johnston, S.T., 2004. The New Caledonia–D'Entrecasteaux orocline and its role in clockwise rotation of the Vanuatu–New Hebrides Arc and formation of the North Fiji Basin. *Special Paper - Geological Society of America* 383, 225–236.
- Johnston, S.T., Acton, S., 2003. The Eocene Southern Vancouver Island Orocline – a response to seamount accretion and the cause of fold-and-thrust belt and extensional basin formation. *Tectonophysics* 365, 165–183.
- Khranov, A.N., 2000. The general magnetostratigraphic scale of the Phanerozoic. In: Zhamoïda, A.I. (Ed.), *Supplement to the Stratigraphic Code of Russia*. St. Petersburg, Transactions of VSEGEI, pp. 24–45 (in Russian).
- Khranov, A.N., Goncharov, G.I., Komissarova, R.A., Osipova, E.P., Pogarskaya, I.A., Rodionov, V.P., Stausilais, I.P., Smirnov, L.S., Forsh, N.N., 1974. Paleozoic paleomagnetism. *Transaction of VNIIGRI, Leningrad*, pp. 1–238 (in Russian).
- Kirschvink, J.L., 1980. The least-square line and plane and the analysis of palaeomagnetic data. *Geophysical Journal of the Royal Astronomical Society* 62, 699–718.
- Klishевич, V.L., Kramov, A.N., 1993. Reconstruction of Turkestan paleocean (southern Tien Shan) for the Early Devonian. *Geotectonics* 4, 66–75 (in Russian).
- Koshkin, V. Ya., 1980. Upper Paleozoic stratigraphy of the northern part of the Balkhash–Ili Hercinian volcanic belt and the Sayak marine basin. *Geophysical Journal of the Royal Astronomical Society* 62, 699–718 (in Russian).
- Kravchinsky, V.A., Konstantinov, K.M., Courtillot, V., Savrasov, J.I., Valet, J.-P., Cherniy, S.D., Mishenin, S.G., Parasotka, B.S., 2002. Palaeomagnetism of East Siberian traps and kimberlites: two new poles and palaeogeographic reconstructions at about 360 and 250 Ma. *Geophysical Journal International* 148, 1–33.
- Kurchavov, A.M., 1994. The lateral variability and evolution of orogenic volcanism in the fold belts. *Geotectonics* 28, 3–18.
- Levashova, N.M., Degtyarev, K.E., Bazhenov, M.L., Collins, A.Q., Van der Voo, R., 2003. Permian paleomagnetism of East Kazakhstan and the amalgamation of Eurasia. *Geophysical Journal International* 152, 677–687.
- Levashova, N.M., Mikolaichuk, A.V., McCausland, P.J.A., Bazhenov, M.L., Van der Voo, R., 2007. Devonian paleomagnetism of the North Tien Shan: implications for the middle–late Paleozoic paleogeography of Eurasia. *Earth and Planetary Science Letters* 257, 104–120.
- Levashova, N.M., Van der Voo, R., Abrajevitch, A.V., and Bazhenov, M.L., in press. Paleomagnetism of mid-Paleozoic subduction-related volcanics from the Chingiz Range in NE Kazakhstan: the evolving paleogeography of an amalgamating Eurasian continent. *Geological Society of America Bulletin*.
- Lister, G.S., Forster, M.A., Rawling, T.J., 2001. Episodicity during orogenesis. In: Miller, J.A., Holdsworth, R.E., Buick, Ian S., Hand, Martin (Eds.), *Continental Reactivation and Reworking*. Geological Society Special Publications, vol. 184, pp. 89–113.
- McFadden, P.L., McElhinny, M.W., 1988. The combined analysis of remagnetization circles and direct observations in paleomagnetism. *Earth and Planetary Science Letters* 87, 161–172.
- McFadden, P.L., McElhinny, M.W., 1990. Classification of the reversal test in paleomagnetism. *Geophysical Journal International* 103, 725–729.
- Menning, M., Alekseev, A.S., Chuvashov, B.I., Davydov, V.I., Devuyt, F.X., Forke, H.C., Grunt, T.A., Hance, L., Heckel, P.H., Izokh, N.G., Jin, Y.G., Jones, P.J., Kotlyar, G.V., Kozur, H.W., Nemyrovska, T.I., Schneider, J.W., Wang, X.D., Weddige, K., Weyer, D., Work, D.M., 2006. Global time scale and regional stratigraphic reference scales of central and west Europe, east Europe, Tethys, south China, and North America as used in the Devonian–Carboniferous–Permian Correlation Chart 2003 (DCP 2003). *Palaeogeography, Palaeoclimatology, Palaeoecology* 240 (1–2), 318–372.
- Menning, M., Katzung, G., Luetzner, H., 1988. Magnetostratigraphic investigations in the Rotliegendes (300–252 Ma) of Central Europe. *Zeitschrift fuer Geologische Wissenschaften* 16 (11–12), 1045–1063.
- Miasnikov, A.K., 1974. Upper Paleozoic of Bakanas Synclinorium (North-East Balkhash area). In: Abdulin, A.A. (Ed.), *Stratigraphy of Devonian, Carboniferous and Permian in Kazakhstan*. Izdatel'stvo Nauka Kazahskoi SSR, Alma-Ata, pp. 154–161 (in Russian).
- Mossakovsky, A.A., Ruzhentsev, S.V., Samygin, S.G., Kheraskova, T.N., 1993. Central Asian fold belt: geodynamic evolution and formation. *Geotectonics* 27 (6), 3–32.
- Natal'in, B.A., Şengör, A.M.C., 2005. Late Palaeozoic to Triassic evolution of the Turan and Scythian platforms: the pre-history of the palaeo-Tethyan closure. *Tectonophysics* 404, 175–202.
- Ogg, J.G., 1995. Magnetic polarity time scale of the Phanerozoic. *AGU Reference Shelf* 1, 240–270.
- Pavlov, V.E., Courtillot, V., Bazhenov, M.L., Veselovsky, R.V., 2007. Paleomagnetism of the Siberian traps: new data and a new overall 250 Ma pole for Siberia. *Tectonophysics* 443, 72–92.
- Puchkov, V.N., 2002. Paleozoic evolution of the east European continental margin involved in the Uralide orogeny. *American Geophysical Union, Geophysical Monograph* 132, 9–31.
- Sal'menova, K.Z., Koshkin, V.Y., 1990. *Stratigraphy and Flora of the Late Paleozoic in the North Balkhash Area*. Nauka, Almaty. 160 pp. (in Russian).
- Şengör, A.M.C., Natal'in, B.A., 1996. Paleotectonics of Asia: fragments of a synthesis. In: Yin, A., Harrison, M. (Eds.), *The Tectonic Evolution of Asia*. Cambridge Univ. Press, Cambridge, pp. 486–640.
- Şengör, A.M.C., Natal'in, B.A., Burtman, V.S., 1993. Evolution of the Altaid tectonic collage and Palaeozoic crustal growth in Eurasia. *Nature (London)* 364, 299–307.
- Skrinnik, L.I., Horst, V.E., 1995. Devonian island arc volcanic complexes in the Junggar Alatau. *Geology and Exploration of Kazakhstan* 4, 6–10.
- Suvorov, A.I., 1963. The Spassk Zone of Central Kazakhstan and Some Problems of Its Strike-Slip Tectonics. *Izvestiya of AN SSSR, seriya geologicheskaya*, vol. 9, pp. 46–50 (in Russian).
- Tauxe, L., Watson, G.S., 1994. The fold test; an eigen analysis approach. *Earth and Planetary Science Letters* 122 (3–4), 331–341.
- Tectonics of Kazakhstan: Explanatory notes to Tectonic map of East Kazakhstan, 1:2 500 000, 1982: Moscow, Nauka, 139 p. (in Russian).
- Tevelev, A.I.V., 2001. The evolution of the south-eastern margin of the Kazakhstan paleocontinent in the Late Paleozoic. In: Milanovsky, E.E., Weinmar, A.B., Tevelev, A.I.V. (Eds.), *Geology of Kazakhstan and the Problems of the Ural–Mongol Fold Belt*. Moscow State University Publications, Moscow, pp. 113–125 (in Russian).
- Tikhomirov, V.G., 1975. Paleozoic Magmatism and Tectonics of Central Kazakhstan. *Nedra, Moscow, USSR (SUN)*, 147 pp. (in Russian).
- Torsvik, T.H., Muller, R.D., Van der Voo, R., Steinberger, B., Gaina, C., in press. Global plate motion frames: toward a unified model. *Reviews of Geophysics*. doi:10.1029/2007RG000227.
- Van der Voo, R., 1993. Paleomagnetism of the Atlantic, Tethys and Iapetus Oceans. Cambridge Univ. Press, Cambridge. 411 pp.
- Van der Voo, R., 2004. Paleomagnetism, oroclines and the growth of the continental crust. *GSA Today* 14 (12), 4–9.
- Van der Voo, R., Levashova, N.M., Skrinnik, L.I., Kara, T.V., Bazhenov, M.L., 2006. Late orogenic, large-scale rotations in the Tien Shan and adjacent mobile belts in Kyrgyzstan and Kazakhstan. *Tectonophysics* 426, 335–360.
- Veimarn, A.B., Milanovsky, E.E., 1990. Famennian Rifting in Central Kazakhstan and Some Other Areas, Paper 1. *Byul. Moskovskogo Obschestva Ispatatelei Prirody, otd. geol.*, vol. 65, pp. 34–47 (in Russian).
- Wang, B., Chen, Y., Zhan, S., Shu, L.S., Faure, M., Cluzel, D., Charvet, J., Laurent-Charvet, S., 2007. Primary Carboniferous and Permian paleomagnetic results from the Yili Block (NW China) and their implications on the geodynamic evolution of Chinese Tianshan Belt. *Earth and Planetary Science Letters* 263, 288–308.
- Watson, G.S., 1956. A test for randomness. *Monthly Notes of the Royal Astronomical Society* 7, 160–161.
- Weil, A.B., Sussman, A.J. (Eds.), 2004. *Orogenic Curvature: Integrating Paleomagnetic and Structural Analyses*. Geological Society of America Special Paper, vol. 383, p. 271.
- Windley, B.F., Alexeiev, D., Xiao, W.J., Kröner, A., Badarch, G., 2007. Tectonic models for accretion of the Central Asian Orogenic Belt. *Journal of the Geological Society (London)* 164, 31–47.
- Yakubchuk, A., 1997. Kazakhstan. In: Moores, Fairbridge (Eds.), *Encyclopedia of European and Asian Regional Geology*. Chapman and Hall, London, pp. 450–465.
- Zijderveld, J.D.A., 1967. AC demagnetization of rocks: analysis of results. In: Collinson, D.W., Creer, K.M. (Eds.), *Methods in Paleomagnetism*. Elsevier, Amsterdam, pp. 254–286.
- Zonenshain, L.P., Kuzmin, M.I., Natapov, L.M., 1990. Geology of the USSR: a plate tectonic synthesis. In: Page, B.M. (Ed.), *American Geophysical Union, Geodynamic series*, vol. 21. Washington, D.C., 250 pp.